The VAB-1 Eph receptor tyrosine kinase and SAX-3/Robo neuronal receptors function together during *C. elegans* embryonic morphogenesis

Simona Ghenea, Jeffrey R. Boudreau, Nicholas P. Lague and Ian D. Chin-Sang*

Department of Biology, Queen's University, Kingston, Ontario K7L 3N6, Canada
*Author for correspondence (e-mail: chinsang@biology.queensu.ca)

Summary

Mutations that affect the single *C. elegans* Eph receptor tyrosine kinase VAB-1 cause defects in cell movements during embryogenesis. Here, we provide genetic and molecular evidence that the VAB-1 Eph receptor functions with another neuronal receptor, SAX-3/Robo, for proper embryogenesis. Our analysis of *sax-3* mutants shows that SAX-3/Robo functions with the VAB-1 Eph receptor for gastrulation cleft closure and ventral epidermal enclosure. In addition, SAX-3 functions autonomously for epidermal morphogenesis independently of VAB-1. A double-mutant combination between *vab-1* and *slt-1* unmasks a role for the SLT-1 ligand in embryogenesis. We provide evidence for a physical interaction between the VAB-1 tyrosine kinase domain and the juxtamembrane and CC1 region of the SAX-3/Robo receptor. Gene dosage, non-allelic non-complementation experiments and co-localization of the two receptors are consistent with a model in which these two receptors form a complex and function together during embryogenesis.

Key words: Eph Receptor Tyrosine Kinase, Robo receptor, Morphogenesis, Cell movements, *C. elegans*, Synthetic lethal

Introduction

Cell movements are crucial for the development of all embryos. If cells are not correctly positioned in the developing embryo, tissues or organs may not be formed or they may be formed in the wrong place or at the wrong time. Cells can navigate to their correct position by sensing their environment for positional cues. In *C. elegans*, the VAB-1 Eph receptor tyrosine kinase and its ephrin ligand EFN-1 function primarily as guidance cues on neuroblasts for proper neuronal and epidermal cell movements (Chin-Sang et al., 1999; George et al., 1998). The vertebrate Eph receptor tyrosine kinases (RTKs) and their ligands, the ephrins, have diverse roles during development. These include axon guidance, angiogenesis and the regulation of cancer (reviewed by Adams and Klein, 2000; Dodelet and Pasquale, 2000; Drescher, 2000; Flanagan and Vanderhaeghen, 1998; Kullander and Klein, 2002). Understanding how the vertebrate Eph receptors signal during development is under intense research, but the large number of receptors and ephrin ligands, as well as the promiscuity of their binding partners, can complicate the picture. By contrast, *C. elegans* has only one Eph RTK and four ephrin ligands.

Null mutations in either the *vab-1* Eph RTK or *efn-1* ephrin result in defective cell movements, and, as a result, the embryos usually die or have severe morphogenesis defects (Chin-Sang et al., 1999; George et al., 1998). However, the fact that the penetrance of the lethality is not complete suggests that there is genetic redundancy in *C. elegans* Eph RTK signaling, that is, other signaling pathways may work together or in parallel with the VAB-1 Eph RTK. Indeed a divergent ephrin, EFN-4,

and a leukocyte common antigen-related (LAR) receptor protein tyrosine phosphatase (RPTP), PTP-3, work redundantly, or in parallel, with the VAB-1 Eph RTK (Chin-Sang et al., 2002; Harrington et al., 2002).

We report that the VAB-1 Eph RTK shows a dosage-dependent genetic interaction with the conserved axon guidance receptor, SAX-3/Robo. The Roundabout (Robo) family of receptors are evolutionary conserved and have been implicated in mediating axon guidance events, specifically axon repulsion upon binding its ligand Slit (Brose et al., 1999; Challa et al., 2001; Kidd et al., 1998; Lee et al., 2001; Seeger et al., 1993; Zallen et al., 1998) (for a review, see Wong et al., 2002). Like the vertebrate and *Drosophila* counterparts, the *C. elegans* Robo homolog SAX-3 is required for multiple axon guidance events, including midline crossing, ventral guidance and nerve ring positioning (Zallen et al., 1999; Zallen et al., 1998). However, the role of SAX-3 in early embryonic cell movements has not been described. Four-dimensional video microscopy revealed that *sax-3* embryos display defects in neuroblast gastrulation cleft closure, as well as ventral movements of the epidermal cells, during ventral closure, similar to those observed in the *vab-1* (Eph RTK) and *efn-1* (Ephrin) mutants. *sax-3* mutants also display epidermal phenotypes that are not observed in *vab-1* mutants, and we provide evidence for a role of SAX-3 in the morphogenesis of epidermal cells independently of VAB-1. We report that double-mutant combinations in *sax-3* and *vab-1* display a completely penetrant embryonic lethal phenotype. Furthermore, double-mutant combinations between *vab-1* and

slt-1, the ligand for SAX-3, show significantly enhanced cell migration defects in comparison with *vab-1* single mutants, revealing a role for SLT-1 in embryogenesis. We also show that the VAB-1 tyrosine kinase binds to the intracellular portion of SAX-3, specifically at the juxtamembrane and CC1 (conserved cytoplasmic region 1) region. The SAX-3 receptor and VAB-1 Eph RTK are co-expressed on a subset of neuroblasts, which is consistent with these two receptors forming a complex. Our results suggest that SAX-3/Robo and VAB-1 can act together to regulate early neuroblast movements and axon guidance.

Materials and methods

Genetic analysis

C. elegans strains were cultured as described by (Brenner, 1974) at 20°C unless noted. Mutants used in this study were as follows.

Chromosome II: *vab-1 (e2, e699, dx31)* (George et al., 1998); *ptp-3 (op147)* (Harrington et al., 2002); *mec-7::gfp (muIs32)* a GFP marker for mechanosensory neurons (gift from Dr C. Kenyon's lab).

Chromosome IV: *efn-4(bx80)* (Chin-Sang et al., 2002); *ajm-1::gfp (jcIs1)* (Mohler et al., 1998).

Chromosome X: *sax-3(ky123)*, the *ky123* allele deletes the signal sequence and the first exon and is likely to be a null allele (Zallen et al., 1998); *slt-1(eh15)*, the *eh15* allele is a duplication of the *slt-1* locus with an out-of-frame deletion in both copies (Hao et al., 2001).

Rearrangement: *mIn1[mIs14 dpy-10 (e128)] II* (Edgley and Riddle, 2001); *mIn1 mIs14* (a.k.a. *mIn1GFP* throughout this paper) is a dominant green fluorescent protein (GFP) balancer for chromosome II, including the region of *vab-1* and *ptp-3*.

Mutations not referenced here can be found elsewhere (Riddle et al., 1997). All *C. elegans* strains were obtained from the *C. elegans* Genetics Stock Center, care of T. Stiernagle (University of Minnesota).

Double-mutant constructs

vab-1(weak); sax-3 double mutants were completely inviable and were maintained as balanced strains of the genotype *vab-1(e2 or e699)/mIn GFP; sax-3(ky123)*. These strains segregate only viable GFP animals, as non-GFP animals (*vab-1; sax-3*) are dead. Balanced strains with the *vab-1(dx31)* null could not be maintained because of the *vab-1* dosage effect (see below). *efn-4; sax-3* double homozygotes were maintained as homozygous lines balanced by an extrachromosomal array (*juEx350*) carrying wild-type copies of *vab-1* and *efn-4* (Chin-Sang et al., 2002). *ptp-3; sax-3* double mutants were analyzed from balanced strains of genotype *ptp-3/mIn1GFP; sax-3*. The penetrance of lethality and morphogenetic defects were quantified as described previously (George et al., 1998).

Dosages studies between the *vab-1* and *sax-3* genes

vab-1 males were crossed to *mIn1GFP/+; sax-3(ky123)* animals to obtain *vab-1/mIn1GFP; +/sax-3* GFP cross progeny. GFP-positive *sax-3* animals were picked based on the Sax-3 notched-head phenotype (*vab-1/mIn1GFP; sax-3*). We were able to isolate *vab-1(dx31)/mIn1GFP; sax-3(ky123)* from *vab-1/mIn1GFP(+); +/sax-3* mothers because *sax-3* animals exhibited maternal rescue. In the subsequent generations, only *mIn1GFP; sax-3* animals were observed, which is consistent with *sax-3* animals requiring two copies of the *vab-1* gene to survive. Of 35 putative *vab-1/mIn GFP; sax-3(ky123)* GFP notched-head animals, four were of the genotype *vab-1/mIn1GFP;+/sax-3(ky123)* double heterozygous and therefore displayed non-allelic non-complementation for the notched-head phenotype. Note that *vab-1* does not show dominant phenotypes and is completely recessive (i.e. +/*vab-1(dx31)*, 100% of embryos viable, *n*>500). To confirm that even in the presence of one copy of the wild-type *vab-1* gene the *sax-3* animals are inviable, we crossed *vab-1(dx31)/mIn1GFP* males to *sax-3(ky123)* animals and scored for the

male cross progeny. Of >100 male cross progeny scored, only GFP animals (+/*mIn1GFP; 0/sax-3*) were observed, suggesting that the non-GFP *vab-1(dx31)/+; 0/sax-3* males were dead. Other crosses using GFP-marked *vab-1* males confirmed this result (see below).

Double heterozygous *+/vab-1; +/sax-3* combinations

Double heterozygous *+/vab-1; +/sax-3* animals were constructed by crossing GFP-marked *vab-1* chromosome (*vab-1 (dx31) GFP (mec-7:gfp muIs32)*) males to *sax-3* females (animals feminized by feeding RNAi with *fem-1*) and *+/vab-1(dx31) GFP; + or 0 /sax-3(ky123)* cross progeny was identified as GFP-positive animals. All cross progeny (GFP positive) that survived developed as hermaphrodites, suggesting that the males were dead. 57% of the GFP embryos were dead (assume that 50% should be XO male embryos), suggesting that about 7% of the XX double heterozygous animals were dead (*t*-test compared with control cross, *P*<0.001). A control cross of *mec-7::GFP* males crossed to *sax-3* females produced male and hermaphrodite survivors, and 27% of the GFP cross-progeny embryos were dead. To score the doubly heterozygous *+/vab-1; +/sax-3* for amphid neuron defects, we crossed *vab-1(dx31)* males to *mIn1GFP; sax-3(ky123)* hermaphrodites to isolate *vab-1/mIn1GFP; +/sax-3*. These animals were stained with the fluorescent dye DiI (Molecular Probes/Invitrogen) and scored for axon guidance defects (lack of ventral guidance or anterior positioning, 25%, *n*=87), as described previously (Zallen et al., 1999).

Yeast two-hybrid assays

Yeast were grown on standard complete and selective media, as appropriate (Sherman, 1991). Yeast transformation was performed using a lithium acetate method (Schiestl and Gietz, 1989). For deletion analysis, pGBKT7 and pGADT7 (Clontech) were used as bait and prey cloning vectors, respectively, and β-galactosidase activity was measured qualitatively by X-GAL overlay assays (Serebriiskii and Golemis, 2000), or was quantified by liquid β-galactosidase (Ausubel et al., 1989). At least three independent liquid β-galactosidase experiments were performed, and the mean and standard error of the mean (s.e.m.) were calculated. The VAB-1 kinase domain (669aa-985aa) was cloned into the pGBKT7 GAL-4 DNA-binding domain vector. SAX-3 deletion constructs were made in pGADT7 by cloning cDNA (PCR derived) encoding the various SAX-3 regions, and their sequence was verified. Amino acid sequences correspond to the SAX-3B isoform (Wormbase Release WS130). Primer sequences and details of plasmid constructs are available upon request.

GST pull-down assays

We used a GST 'pull-down' assay to confirm the SAX-3/VAB-1 interaction. A cDNA encoding the *vab-1* intracellular region (581aa-1117aa) was cloned in frame to Glutathione-S-Transferase (pGEX4T-2, Amersham), expressed in *E. coli* (BL21 Tuner) and purified on glutathione agarose beads (GST-Bind, Novagen), according to the manufacturer's protocol. A cDNA encoding the SAX-3 juxtamembrane to CC1 region (900aa-1030aa) was fused in-frame to Maltose-Binding Protein (pMALp2x, New England Biolabs) and expressed in *E. coli*. Soluble extract containing MBP-SAX-3 (Load) was incubated overnight at 4°C with either GST (3 mg/ml) or GST-VAB-1 (0.25 mg/ml) bound to 100 μl beads. Unbound fractions were collected, protein bound to beads was washed three times [25 mM HEPES (pH 7.5) 250 mM NaCl, 5% glycerol, 0.05% Triton-X-100] and a proportional loading of each sample was analyzed by SDS-PAGE followed by western blotting. MBP-SAX-3 was detected by using anti-MBP (New England Biolabs) and secondary HRP-anti-rabbit antibodies (Upstate) followed by ECL (Pharmacia Biotech).

Immunohistochemistry

Fixation and staining of embryos was performed as described previously (Chin-Sang et al., 1999; Finney and Ruvkun, 1990). Chicken polyclonal antibodies against GFP (Chemicon) were used at

1:200 dilutions. Rabbit anti-VAB-1 antibodies (antigen: VAB-1-6XHIS intracellular 581aa-1117aa) were used at 1:100 dilutions. MH27 monoclonal antibody (Francis and Waterston, 1991) (anti-AJM-1) was used at a concentration of 1:500. Rhodamine-conjugated goat anti-mouse (Chemicon), FITC-conjugated goat anti-chicken, and Texas Red-conjugated goat anti-rabbit secondary antibodies (Jackson ImmunoResearch Laboratories) were used at 1:500 dilutions.

Transgenic rescue and reporter constructs

To create a rescuing SAX-3::GFP reporter (*quEx89*), we used a PCR fusion-based approach (Hobert, 2002) to generate a PCR (Roche Expand Long PCR) product consisting of 1.2 kb of the *sax-3* promoter, the *sax-3* genomic region (exons 1-5) followed by the rest of the *sax-3* cDNA fused in frame to GFP and *unc-54* 3′UTR sequences derived from pPD95.75 (Dr A. Fire's laboratory). A final 10.4 kb PCR product (10 ng/µl) was co-injected with pRF4 (30 ng/µl) marker and transgenics were obtained as described (Mello et al., 1991). The SAX-3 minigene (*quEx99*) consisted of 1.5 kb of the *sax-3* promoter fused to the whole 3.8 kb *sax-3* cDNA and followed by 0.7 kb of the *sax-3* 3′UTR. The final mini-gene PCR product was co-injected with *odr-1*::RFP transformation marker (gift from Dr C. Bargmann's Laboratory). For *ajm-1*::SAX-3 (*quEx100*) and *F25B3.3*::SAX-3 (*quEx102*), we used the same strategy as for the mini-gene, where *sax-3* promoter sequence was replaced with 1.6 kb sequence of *ajm-1* promoter and 1.5 kb sequence of *F25B3.3* promoter, respectively. The *vab-1* rescuing mini-gene (pCZ47) was as described previously (George et al., 1998).

4D video microscopy

4D video microscopy was carried out essentially as described previously (Chin-Sang et al., 2002). Recordings were made at room temperature (22°C) using a Zeiss Axioplan 2 microscope with a 63× Plan-neofluar objective lens, Axiocam and Axiovison software. Fifteen to twenty (0.5 to 1 µm) z sections were taken at 1-2 minute intervals throughout development. We recorded 20 *sax-3(ky123)* embryos of which 10 did not complete embryogenesis. For time-lapsed imaging of GFP-expressing embryos, we replaced the standard UV (100 W Mercury short arc burner) lamp with a 250 W Halogen fiber-optic cold light source (Zeiss KL2500 LCD). Images were captured every 5-8 minutes.

Results

sax-3 and *vab-1* are synthetic lethal and display gene-dose sensitivity

The incomplete penetrance of the embryonic lethality of *vab-1* suggested that other genes function with *vab-1* during embryogenesis. We identified *sax-3* in a candidate gene screen for genes that are synthetic lethal with *vab-1* (S.G. and I.D.C.-S., unpublished). We observed 48% embryonic lethality for *sax-3(ky123)*, n=1210, and 54% embryonic lethality for *vab-1(dx31)*, n=1065 (Fig. 1). We made double-mutant combinations with a putative null allele of *sax-3(ky123)* (Zallen et al., 1998) and various alleles of *vab-1* [*e2, e699, dx31*; weak, intermediate and strong (null), respectively] (George et al., 1998). All *vab-1* alleles showed 100% embryonic lethality with *sax-3(ky123)*, and the weak *vab-1* alleles showed a synergistic interaction with *sax-3*, as the lethality was more than additive (Fig. 1).

In the course of making double-mutant combinations with *vab-1* and *sax-3/Robo*, we identified a gene-dosage dependence of *vab-1* in that +/*vab-1(dx31); sax-3* heterozygotes were completely inviable (see Materials and methods). We also confirmed the gene dosage requirement for *vab-1* by crossing
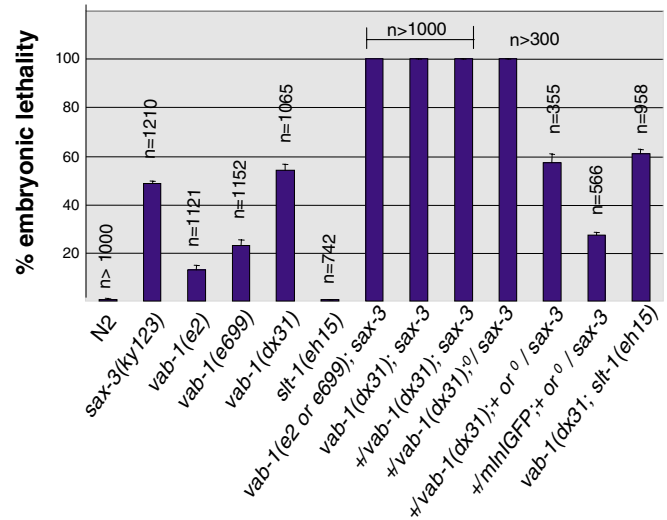
Fig. 1. *vab-1/Eph* is synthetic lethal with *sax-3/Robo* and displays gene-dose sensitivity. The percentage embryonic lethality of single mutants and double mutant combinations between *vab-1*, *sax-3* and *slt-1* is shown. All alleles of *vab-1* tested are 100% embryonic lethal with the *sax-3(ky123)* null. The null allele of *vab-1(dx31)* displays a dosage sensitivity with *sax-3* in that embryos are dead even in the presence of one wild-type copy of *vab-1*. +/*dx31; 0/sax-3* males are also dead. The double heterozygous embryos +/*dx31; + or 0/sax-3* includes hermaphrodites and males, and the lethality is greater than 50% (57%), suggesting some non-allelic, non-complementation. By contrast, control crosses + or 0/*sax-3* gave 27% embryonic lethality. *vab-1; slt-1* does not display synthetic lethality but the phenotypes are enhanced. Error bars represent s.e.m. of at least three broods; *n*, total number of embryos scored for each genotype.

vab-1(dx31) males to *sax-3* animals. Because *sax-3* is on the X chromosome, half of the cross progeny should be +/*vab-1(dx31); 0/sax-3* (males) and the other half +/*vab-1(dx31); +/sax-3* (hermaphrodites). From several independent crosses, all cross progeny developed as hermaphrodites, suggesting that heterozygous +/*vab-1; 0/sax-3* males die as embryos (Fig. 1). Therefore, removing just one copy of the *vab-1* gene reveals an essential role for *sax-3* during embryogenesis. The double heterozygous +/*vab-1; + or 0/sax-3* embryos (hermaphrodites and males) from *vab-1* crossed to *sax-3* displayed greater than 50% lethality. Furthermore, +/*vab-1(dx31); +/sax-3(ky123)* showed weak penetrance notched-head phenotypes, demonstrating non-allelic non-complementation (see Materials and methods).

If VAB-1 functions with the SAX-3 receptor during embryogenesis, we reasoned that *sax-3* mutations may also show a synthetic lethal phenotype with other genes known to function with *vab-1*. Two proteins have been shown to function redundantly with VAB-1 Eph RTK signaling during embryonic morphogenesis: PTP-3, a LAR (Leukocyte Common Antigen Related) Receptor Tyrosine Phosphatase (Harrington et al., 2002) and EFN-4 a divergent Ephrin (Chin-Sang et al., 2002). We made double mutants between *sax-3(ky123)* and *ptp-3(op147)* or *efn-4(bx80)*. As predicted, double-mutant combinations caused 100% embryonic lethality. Unlike *vab-1*, we did not see any gene dosage effects or non-allelic non-complementation with either *ptp-3* or *efn-4* mutants. The embryonic lethality appears to be caused by defects in

neuroblasts and epidermal movements similar to those seen in the *vab-1 ptp-3* and *vab-1; efn-4* double mutants, respectively (Chin-Sang et al., 2002; Harrington et al., 2002) (Fig. 2G). Both *ptp-3* and *efn-4* single mutations have very modest embryonic lethality (10% and 14%, respectively), therefore *sax-3* mutations act synergistically with *ptp-3* and *efn-4*.

Because it is possible that VAB-1 and SAX-3 may function

together during axon guidance, we asked whether these two genes display a gene-dosage interaction, as seen in the embryonic lethality phenotype. We show that the double-heterozygous +/*vab-1*; +/*sax-3* animals display defects in axon guidance in head neurons. Twenty-five percent of the double heterozygous animals displayed an anterior positioning and/or defects in ventral guidance of the amphid neurons similar to

Fig. 2. *sax-3* mutants display defects in cell movements similar to those seen in *vab-1* embryos. (A) Cartoon of wild-type *C. elegans* embryogenesis highlighting some cell movement events during embryogenesis. The gastrulation cleft is closed by lateral neuroblast movements by 200 minutes, and enclosure of the ventral epidermis (red cells) is observed by 325 minutes at 22°C. Lateral (seam cells) are coloured yellow and the dorsal epidermis is coloured orange. Arrows show the direction of cell movements. (B-G) Embryogenesis of N2 (wild type) and various single- and double-mutant combinations. Images are single frames taken from 4D DIC movies of individual embryos. All embryos are shown as ventral views; anterior is to the left. The times are given in minutes relative to the first cleavage, and are shown at the bottom left of each panel. Scale bar: 10 µm. (B) In wild-type (*wt*) development the ventral gastrulation cleft is small (<15 µm, dotted line). After the cleft is closed, the epidermal cells migrate around the embryo to meet at the ventral midline. The leading cells are marked (arrows). (C) *sax-3(ky123)* embryos have broader, deeper and more persistent gastrulation clefts because the neuroblasts either fail to move or migrate abnormally. Later when the epidermal cells start to migrate the gastrulation cleft is still open and it is common to see cells 'floating' (asterisk) around in the still open gastrulation cleft. The open gastrulation cleft and wandering cells may interfere with the epidermal leading cells (arrows) and posterior pocket cells enclosing the embryo. The embryo usually ruptures at the ventral side during the elongation process. (D) *vab-1(dx31)* is shown for comparison. (E) Double-mutant *vab-1(e2); sax-3(ky123)* embryos have cell movement defects that are similar to the phenotypes of either *vab-1* or *sax-3* single mutants. The gastrulation cleft is usually larger and less defined, as the cells are disorganized (Class I, strongest phenotype). (F) Double-mutant *vab-1(dx31); slt-1(eh15)* embryos have broader, deeper and more persistent gastrulation clefts. Epidermal cells are highly disorganized and do not migrate to the ventral side, and the embryos usually arrest before ventral enclosure; a phenotype not seen in either of the single mutants. (G) Double mutants *efn-4(bx80); sax-3(ky123)* are completely inviable and display cell movement defects that are similar to those of the *vab-1 ptp-3* and *vab-1(dx31); efn-4(bx80)* double mutants. The question mark denotes that the embryo was so disorganized that we could not confidently identify whether this cell was the leading cell. *ptp-3(op147); sax-3(ky123)* also exhibited similar defects (not shown).
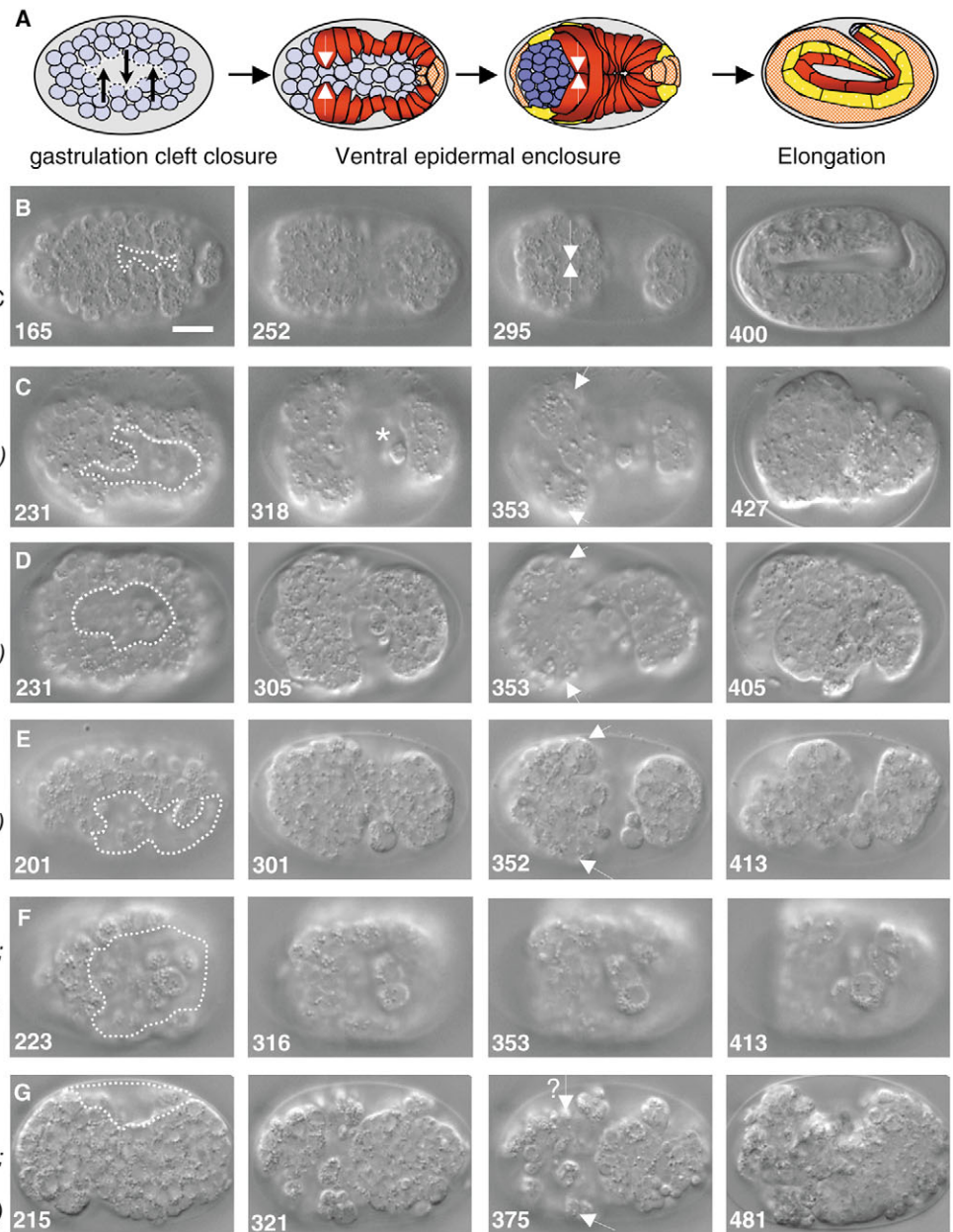
the phenotype of *sax-3* mutant animals (Fig. 3). Thus, *vab-1* and *sax-3* show non-allelic non-complementation in axon guidance.

sax-3 mutants have defects in neuroblast and epidermal cell movements that are similar to those of *vab-1* mutants

We used four-dimensional (4D) video microscopy to record the embryonic development in *sax-3* mutant embryos. *sax-3* mutant embryos displayed defects in two phases of embryonic cell movements: closure of the ventral gastrulation cleft by short-range neuroblast movements; and enclosure of the embryo by epidermal cell shape changes, which are similar to those seen in *vab-1* and *efn-1* mutants (Chin-Sang et al., 1999; George et al., 1998). For this reason, they were classified using the same criteria as those used to classify *vab-1* and *efn-1* embryonic phenotypes (see Fig. 2).

In 30% of the *sax-3* embryos examined, the gastrulation cleft remained open at the time of epidermal ventral enclosure and the epidermal cells failed to contact each other at the ventral midline. As a result, the embryos ruptured at the ventral side (Fig. 2C, Class I, strongest phenotype). In 20% of the embryos there were no apparent defects in gastrulation cleft closure, and although the epidermal cells met at the ventral side, they failed to form stable contacts (Class II). These animals also ruptured at the ventral midline. Another striking phenotype displayed

by *vab-1* and *efn-1* mutants was an epidermal notched head, which was most likely caused by improper epidermal ventral enclosure in the anterior region. *sax-3(ky123)* mutant animals also show a 'notched' head phenotype (17% strong notches), similar to that seen in *vab-1* and *efn-1* mutants, which is consistent with *sax-3* exhibiting similar embryonic defects as Eph RTK signaling defective animals (Fig. 5A).

We also examined the lethality of double *vab-1(e2); sax-3(ky123)* mutants. These double-mutant embryos died with the most severe gastrulation cleft defects, in addition to defects in epidermal ventral enclosure (Fig. 2E, Class I). We did not see any new phenotypes in the double mutants that were not observed in the single mutants (other than the frequency of the defects) (Fig. 2E). SLT-1 is predicted to be the only *C. elegans* ligand identified so far for SAX-3 (Hao et al., 2001), and a null mutation in *slt-1* does not display embryonic lethality (Fig. 1). When we examined the *vab-1(dx31); slt-1(eh15)* double mutant, we found 60% embryonic lethality and these embryos arrested during ventral enclosure with a larger gastrulation cleft than *vab-1* single mutants. Often in these animals, the epidermis did not initiate migration toward the ventral side and remained on the dorsal side (Fig. 2F). More cells failed to ingress during gastrulation cleft closure and the posterior pharynx was often abnormal (data not shown). This is a new phenotype, which was not observed in *vab-1*, *sax-3*, or *vab-1; sax-3* mutants, suggesting that SLT-1 has a SAX-3-independent

DIC

Green =GFP (pharynx)
Red = DiI (amphid neurons)
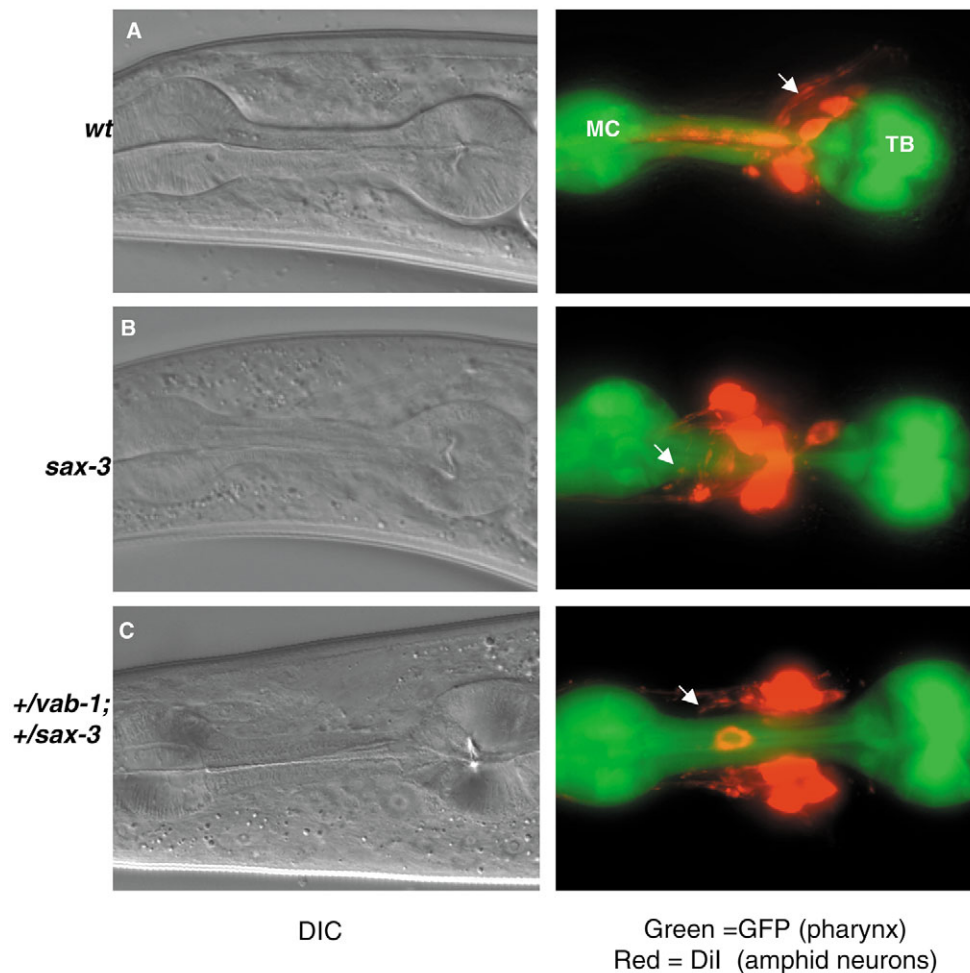
**Fig. 3.** *vab-1* and *sax-3* display non-allelic non-complementation in axon guidance; DIC (left) and fluorescence (right) images of the head region are shown. (A) +/*mIn1GFP* 'wild-type' adults stained with the vital dye DiI to visualize the amphid head neurons (red). The *mIn1GFP* marker was used to visualize the pharynx (green). The amphid neuronal cell bodies are close to the terminal bulb (TB) of the pharynx. The amphids send out axons that first migrate ventrally and then dorsally to project and terminate in the nerve ring (arrow), which is posterior to the metacorpus (MC). (B) +/*mIn1GFP; sax-3* mutants display a highly penetrant anterior axon displacement. The axons project anteriorly past the metacorpus, arrow. In addition, *sax-3* amphid cell bodies are often misplaced more anteriorly. (C) *vab-1/mIn1GFP; +/sax-3* double heterozygous animals display axon guidance defects (25%) similar to those of *sax-3* homozygous animals.

role. Therefore the *vab-1; slt-1* double mutation does not lead to synthetic lethality; however, it can drastically enhance the *vab-1* phenotype and unmasks an embryonic role for *slt-1* in embryonic cell migration (see below). Together, these findings suggest that *sax-3* and *vab-1* have common and partially redundant roles during these morphogenetic cell movements.

sax-3/Robo exhibits epidermal defects not observed in vab-1 mutants

Previously (Chin-Sang et al., 1999; George et al., 1998) suggested that the epidermal cell migration defects seen in ephrin signaling mutants arise from defects in the organization of the neuronal substrate that they migrate over, and not directly from a lack of ephrin signaling in epidermal cells.

Because the DIC time-lapse showed that *sax-3* mutants have similar defects in epidermal cell migration during ventral enclosure, we questioned whether there is the same deficient mechanism that is proposed in ephrin signaling. We analyzed the movement of epithelial cells in greater detail by 4D time-lapse microscopy of an AJM-1::GFP reporter construct and MH27 (anti-AJM-1) antibodies, which localize to adherens junctions of epidermal cells. Wild-type embryos carrying AJM-1::GFP *(jcIs1)* illustrate two epidermal morphogenetic steps that occur at approximately the same time on opposite sides of the embryo: (1) ventral migration of the contralateral pairs of epidermal cells to the ventral midline where they contact one another to wrap the embryo in the epidermal monolayer (Fig. 4A); and (2) intercalation of the two dorsal-
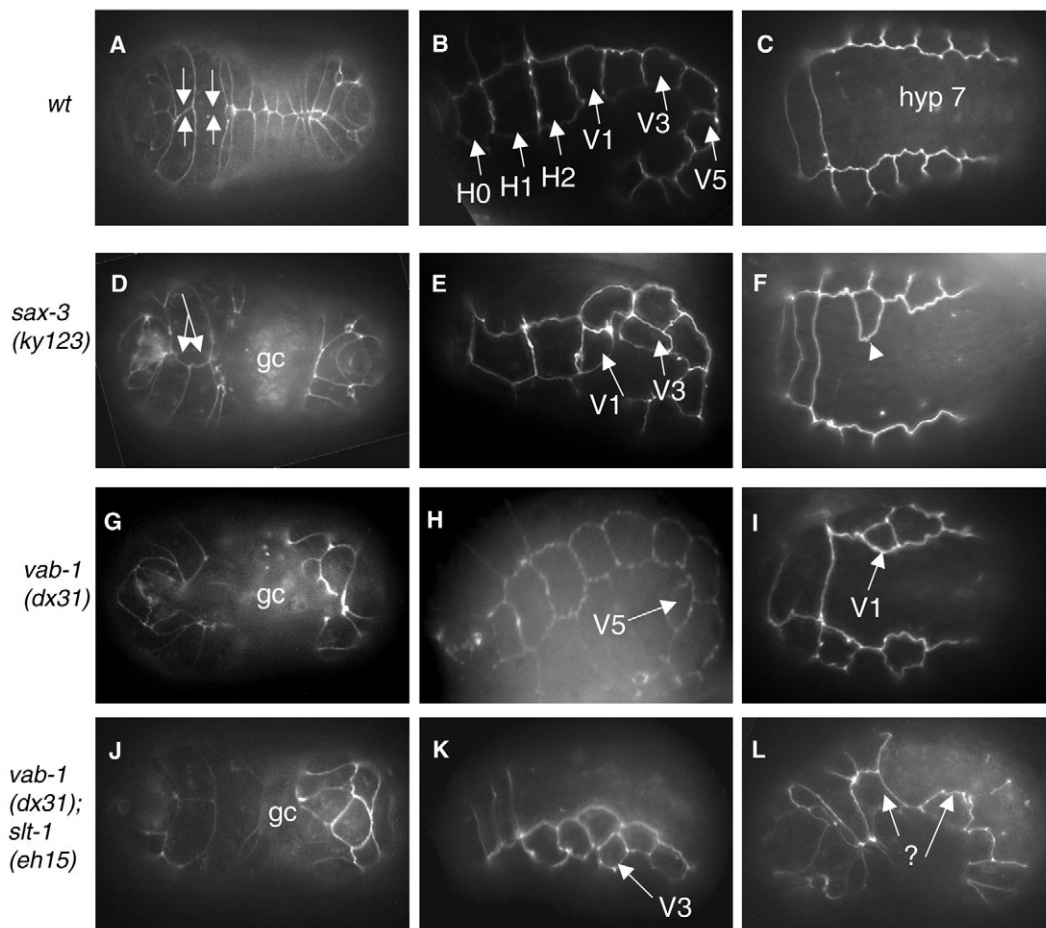
Fig. 4. Epidermal defects in *sax-3(ky123)*, *vab-1(dx31)*, and *vab-1(dx31); slt-1(eh15)* mutants. Columns from left to right show ventral, lateral and dorsal views, with the exception of K and L, which are dorsolateral views. In all panels anterior is to the left. All animals carry the *ajm-1::GFP (jcIs1)* epidermal cell marker. (A-C) Wild-type embryo development. (A) The contralateral epidermal cells meet at the ventral midline and enclose the embryo (arrows point to the leading cell). (B) The seam cells are organized in a lateral row of 10 cells (H0, H1, H2, V1-V6, T). (C) The dorsal epidermal cells fuse to form the hyp 7 syncytium. (D-F) Defects in *sax-3* mutants. (D) One of the left leading cells maintained inappropriate contact (double arrow) with both leading cells on the opposite side. The unclosed gastrulation cleft (gc) prevented the pocket cells from connecting at the ventral midline. (E) The positions of V1 and V3 seam cells are ventrally shifted (arrows), leading to abnormal seam cell contacts. (F) One of the dorsal epidermal cells did not fuse with its neighbours and exists as a single cell within the hyp 7 syncytium (arrowhead). (G-I) Defects in *vab-1* mutants. (G) The unclosed gastrulation cleft (gc) prevented the leading and pocket cells from enclosing the embryo. (H) V5 is shifted ventrally, allowing a direct contact of V4 with V6. (I) No defects are observed for the dorsal epidermis; however, one of the seam cells (V1) is shifted dorsally (arrow), allowing H2 to contact V2. (J-L) Defects in *vab-1; slt-1* double mutants. (J) The ventral epidermis structure is drastically disrupted because of the presence of the enlarged gastrulation cleft (gc). (K) V3 is shifted ventrally (arrow) and the V2 cell makes direct contact to V4. (L) The shape and position of anterior epidermal cells and seam cells are drastically changed. Arrows indicate unidentified (?) seam cells because some appear to fuse to dorsal hyp 7.

most rows of epidermal cells that later fuse to each other and form the dorsal syncytium (Fig. 4C) (Podbilewicz and White, 1994; Williams-Masson et al., 1998). In *sax-3* embryos, AJM-1::GFP was expressed and localized to the junctions of the epidermal cells, as in wild-type embryos. We analysed 45 embryos and we observed three kinds of epidermal defects in *sax-3(ky123)* embryos. The most dramatic defect was the disruption of the migration of the ventral pocket cells due to the lack of underlying substrate cells, caused by the failure of gastrulation cleft closure (13 embryos). In nine of those 13 embryos, the leading cells met at the ventral midline, and, in the other four embryos, the leading ventral epidermal cells failed to migrate or migrated abnormally. These 13 embryos ruptured at the ventral midline and could be classified as Class I, as described for DIC time-lapse above (Fig. 4D). The second defect observed was a change in the shape and position of the dorsal epidermal cells that led to cell intercalation and fusion defects (four embryos; Fig. 4F). In addition, three of these embryos also failed to undergo ventral enclosure. The last defects observed were abnormalities in the lateral epidermis (12 embryos). In *C. elegans* embryos, 10 epidermal cells (H0, H1, H2, V1-V6 and T) form a lateral row of seam cells on each side of the embryo (Fig. 4B). In *sax-3* mutants, one or more seam cells were displaced. For example, V1, V3 and V5 were often shifted ventrally or dorsally, resulting in inappropriate cell contacts between adjacent cells (Fig. 4E). The remaining 16 embryos enclosed and elongated without epidermal defects. In summary, the *sax-3* gene is necessary for at least three different processes during epithelial morphogenesis of the embryo: for ventral epidermal migration, dorsal epidermal cell migration and fusion, and for the alignment of the lateral seam cells. In addition, *sax-3* is required for the neuroblast movements during gastrulation cleft closure.

We also examined *vab-1(dx31)* mutants for AJM::GFP phenotypes found in *sax-3* mutants. As in *sax-3* mutants, the most dramatic defect was the presence of an open gastrulation cleft, which prevented the epidermal cells from migrating and enclosing the embryo (Class 1, 6 out of 20 embryos examined, Fig. 4G). Furthermore, four embryos had no apparent ventral enclosure defects, but eventually ruptured later at the ventral midline. Two embryos had similar seam cell displacements to those observed in *sax-3* embryos. For example, V5 was shifted ventrally, and V4 made direct contact with V6 (Fig. 4H). However, unlike *sax-3* mutants, *vab-1* mutants displayed no defects in the dorsal epidermal cells. By contrast, the *vab-1; slt-1* double mutant did exhibit more severe epidermal defects than those observed in *vab-1* alone. Like in *sax-3* mutants, the epidermal structure was highly disorganized on both ventral (8 out of 22 embryos) and dorsal sides (2 out of 22 embryos; Fig. 4J,L) and more seam cells had abnormal shapes or were displaced than in *vab-1* mutants alone (four embryos) (Fig. 4K,L). Together, these findings indicated that the VAB-1 Eph RTK is required for epidermal morphogenesis but only for a specific subset of cells. Furthermore *vab-1; slt-1* double mutants exhibited phenotypes not exhibited in either of the single mutants, suggesting functional redundancy during epidermal morphogenesis.

SAX-3 functions in both the epidermis and nervous system

Because the dorsal epidermal defects observed in *sax-3*

mutant embryos cannot be easily reconciled by neuroblast signaling (as is proposed for the ventral epidermal defects observed in *vab-1* and *efn-1*), we questioned whether SAX-3 could function cell autonomously in epidermal cells. We expressed SAX-3 specifically in either epidermal or neuronal cells using the *ajm-1* and *F25B3.3* promoters, respectively. SAX-3 tissue-specific expression was scored for its ability to rescue the embryonic lethality of *sax-3* mutants. The *ajm-1* gene is activated only after the epidermal cells are specified and therefore the *ajm-1* promoter is suitable to quantify the activity of SAX-3 in epidermal cells (Mohler et al., 1998). *F25B3.3* is a RAS1 guanine nucleotide-exchange factor that is expressed early in neuroblasts and throughout the adult nervous system (Altun-Gultekin et al., 2001). Both *ajm-1::*SAX-3 and *F25B3.3::*SAX-3 constructs were able to partially rescue the lethality in *sax-3(ky123)* mutant embryos (Fig. 5A), reducing the embryonic lethality from 48% to 23% for *ajm-1::*SAX-3*; sax-3* transgenic animals, and to 17% lethality for *F25B3.3::*SAX-3*; sax-3* transgenic animals, suggesting that the *sax-3* gene functions both in epidermal and neuroblast cells. Surprisingly, the epidermal 'notched-head' phenotype was rescued only by the neuronal *F25B3.3::*SAX-3 construct and not the epidermal *ajm-1::*SAX-3 construct (Fig. 5A).

SAX-3/Robo is expressed in the same neuroblasts as the VAB-1 Eph RTK

SAX-3 expression has been reported in the nervous system, particularly during the stage of axonal outgrowth in the embryo (Zallen et al., 1998). However, we re-examined the SAX-3 expression pattern (specifically in the embryo), and we were able to extend the SAX-3 expression pattern by creating transgenic animals that carried the entire SAX-3 receptor fused to GFP expressed from its own promoter (see Material and methods). The SAX-3::GFP construct was able to partially rescue the *sax-3* embryonic lethality and the notched-head phenotype, suggesting that SAX-3::GFP has functional activity (Fig. 5A). SAX-3::GFP is expressed in early neuroblasts during gastrulation cleft closure and in the underlying neurons during ventral enclosure, similar to VAB-1 and EFN-1. However, unlike VAB-1 or EFN-1, SAX-3::GFP was also observed in epidermal cells (Fig. 5B) (Chin-Sang et al., 1999; George et al., 1998). To examine SAX-3 and VAB-1 co-localization, we used anti-VAB-1 antibodies and anti-GFP antibodies on transgenic embryos expressing VAB-1 (pCZ47) (George et al., 1998) and the SAX-3::GFP construct. VAB-1 and SAX-3 co-localized on neuroblasts, consistent with SAX-3 and VAB-1 functioning together during this stage of development. However, the co-localization is not exact and VAB-1 and SAX-3 were also expressed in separate cells. In general, we found that co-localization of VAB-1 and SAX-3 occurred more frequently in the early neuroblasts, but in later embryos (post-ventral enclosure), we found that SAX-3 and VAB-1 were expressed in separate groups of neighboring cells, reminiscent of the reciprocal expression patterns of ephrin ligands and their receptors (Fig. 5C).

The juxtamembrane and CC1 region of SAX-3/Robo binds the VAB-1 tyrosine kinase

Non-allelic non-complementation or gene-dosage sensitivity

Development *(side text)*

Fig. 5. SAX-3 is expressed in a subset of neuroblasts and neurons that express VAB-1. (A) Extrachromosomal arrays carrying SAX-3/Robo in a *sax-3* background have rescuing activity. We scored for rescue of the *sax-3* embryonic lethality and notched-head phenotype (top right). The transgenic lines restore SAX-3 activity in neuroectoblast (*F25B3.3*::SAX-3), epithelial cells (*ajm-1*::SAX-3) or all SAX-3 tissues (SAX-3 mini gene and SAX-3::GFP). By contrast, the *odr-1*::RFP transgenic marker had no rescuing activity. Note that the *ajm-1*::SAX-3 did not rescue the notched-head phenotype. Complete rescue is not expected, as these transgenic animals carry an extrachromosomal array that is randomly lost during cell divisions, therefore not all animals carry the extrachromosomal array. Error bars indicate s.e.m. from at least three broods; *n*, total number of embryos scored. Asterisks indicate transgenic animals with significantly less embryonic lethality or notched heads than *sax-3* animals (*t*-test, *P*<0.001). Scale bar: 20 μm. (B) SAX-3 is expressed in neurons and in epidermal cells during epidermal ventral enclosure. SAX-3::GFP fluorescence is observed in many neurons (top) and is similar to VAB-1 expression. SAX-3::GFP is also expressed in epidermal cells (bottom). (C) VAB-1 and SAX-3 are co-expressed in some neuroblasts and neurons during development. Three different stages are shown: 100-200 cells (top), pre-ventral enclosure (middle) and comma stage (bottom). Double immunostaining with anti-VAB-1 (red) and anti-GFP (green) was used to visualize the co-localization of VAB-1 and SAX-3. VAB-1 and SAX-3 are expressed in similar cells but their expression patterns are not identical, consistent with these two receptors functioning together in some cells but also having independent roles during development.
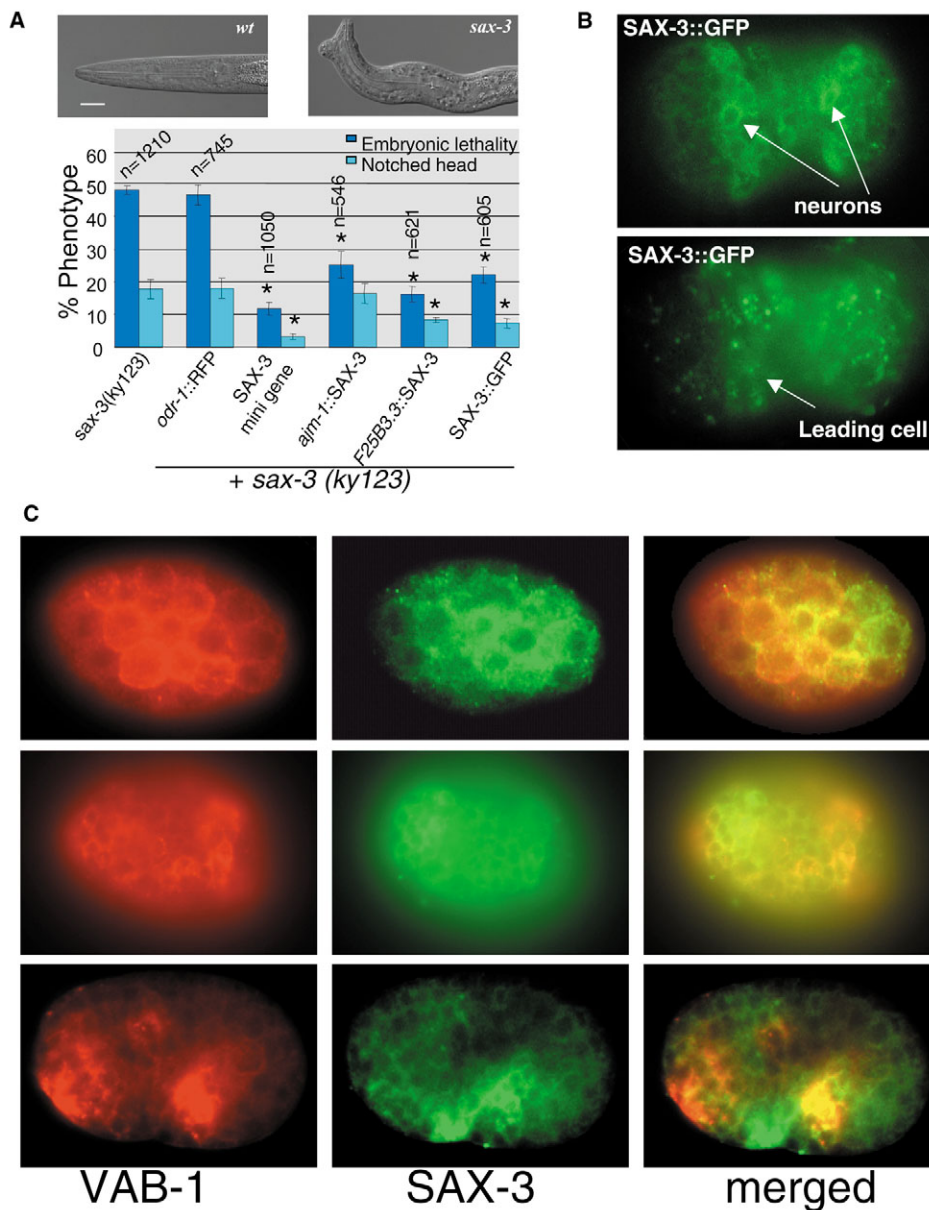
between two genes can be interpreted genetically as two proteins acting in a complex. Because VAB-1 exhibits gene-dose sensitivity with SAX-3 in embryogenesis and in axon guidance, we tested whether these two receptors can physically interact. We used the VAB-1 tyrosine kinase region fused to the GAL-4-binding domain, and the full-length intracellular region of SAX-3 fused to the GAL-4-activation domain, to show that these two proteins can interact in a yeast two-hybrid assay (Fig. 6A,B).

Deletion analysis of the SAX-3 protein determined that the juxtamembrane and CC1 domains of SAX-3/Robo are necessary and sufficient for binding the VAB-1 kinase (Fig. 6B). Neither the juxtamembrane nor the CC1 domain alone showed significant binding to VAB-1, suggesting that both these regions are necessary for the interaction. We further confirmed the interaction between SAX-3 and VAB-1 by Glutathione S-Transferase (GST) pull-down experiments (see

Materials and methods). A fusion protein consisting of Maltose Binding Protein (MBP) fused to the SAX-3 juxtamembrane and the CC1 region (MBP-SAX-3 juxta CC1) specifically co-precipitated with GST-VAB-1 (Fig. 6C).

Discussion

We show that the SAX-3/Robo receptor functions with the VAB-1 Eph RTK in neuronal and epidermal morphogenesis. Time-lapsed video analysis revealed that *sax-3* mutants have similar cell movement defects to those of *vab-1* (Eph RTK) and *efn-1* (Ephrin) mutants. Our genetic, expression pattern and in vitro interaction analyses suggest that SAX-3 and VAB-1 may function together to receive signals on neuroblasts and neurons to regulate cell movements and axon guidance. In addition, SAX-3/Robo has roles in epidermal morphogenesis that function independently of VAB-1.

Fig. 6. The VAB-1 tyrosine kinase domain physically interacts with the juxtamembrane and CC1 region of SAX-3/Robo. (A) Schematic diagrams of the VAB-1 Eph RTK and SAX-3/Robo receptor. VAB-1 Kinase region (669 aa-985 aa) was fused in frame to the GAL-4 DNA-binding domain and used as bait in yeast two-hybrid assays. The SAX-3 intracellular CC1, CC3 and CC2 regions are shown as blue boxes. SAX-3 does not have a recognizable CC0 consensus and CC3 is N terminal to CC2 when compared with other Robo receptors. (B) Deletion constructs of the intracellular portion of SAX-3 were tested for their ability to bind the VAB-1 tyrosine kinase domain. Liquid β-Galalctosidase units and yeast X-GAL overlay assays indicate the quantity of activation (interaction). The juxtamembrane and CC1 region is necessary and sufficient for the interaction with the VAB-1 kinase region (dashed rectangle). (C) GST 'pull-down' experiments confirm that the SAX-3 juxtamembrane and CC1 region (900 aa-1030 aa) is sufficient for the interaction with the VAB-1 intracellular region. MBP-SAX-3 *E. coli* lysates were incubated with GST or GST-VAB-1. MBP-SAX-3 input (Load), unbound (UB) and bound (B) fractions were analyzed by SDS-PAGE and western blotting using anti-MBP to visualize SAX-3. The SAX-3 interaction is specific to GST-VAB-1 and not GST alone. GST-VAB-1 is also specific for MBP-SAX-3, as it does not bind the MBP degradation products (asterisks) in the Load.
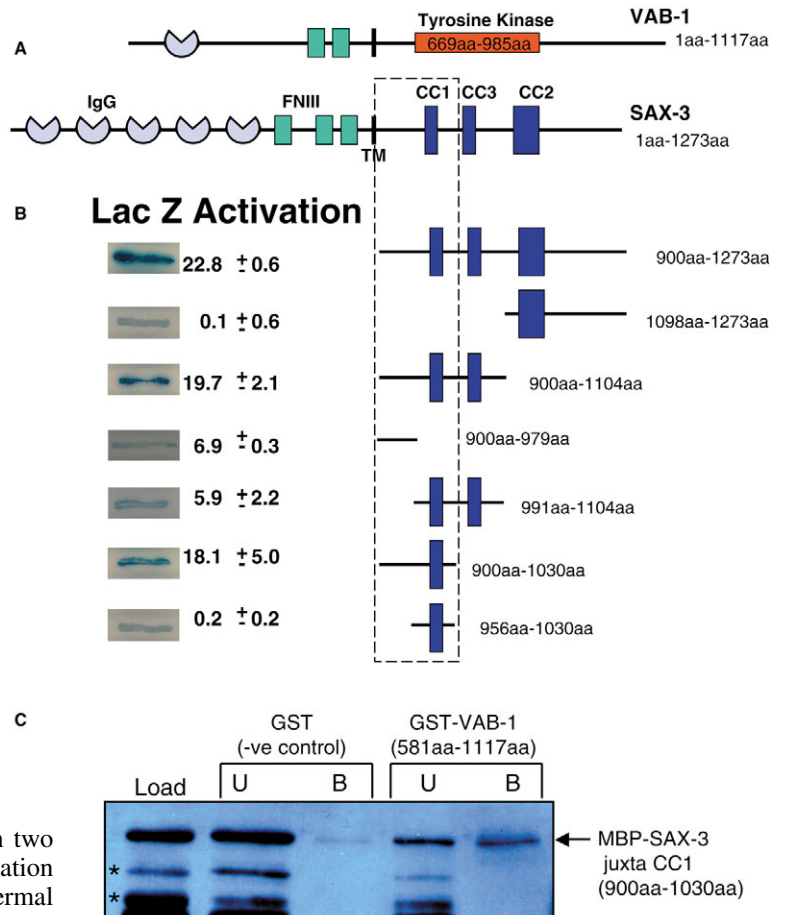
SAX-3 has roles in embryonic cell movements

We report that SAX-3 is necessary for cell migration in two phases of embryonic development, closure of the gastrulation cleft by short-range movement of neuroblasts, and epidermal cell movement during ventral enclosure; defects in cell migration during these two phases are also observed in ephrin-signaling mutants.

In *C. elegans*, cells are generated from a stereotypical cell lineage during embryogenesis. Most of the epidermal cells are descended from the AB founder cell, with the exception of the posterior dorsal epidermal cells, which are derived from the C founder cell (Podbilewicz and White, 1994; Sulston et al., 1983). Our results indicate that *sax-3* mutants have epidermal defects only from cells derived from the AB lineage and not the epidermal C lineage. Previous results showed that SAX-3 has roles in cell positioning and axon guidance. The CAN, and HSN neurons are mispositioned in *sax-3* mutant animals (Zallen et al., 1999). The ALM neuron is also mispositioned in *sax-3* and *slt-1* mutants (Hao et al., 2001). Similarly, *vab-1* animals show defects in CAN and PLM cell positioning (A. Mohamed and I. D. Chin-Sang, unpublished). One simple hypothesis for the epidermal defects observed in *sax-3* embryos is the failure of AB epidermal precursors to reach their final position because of incomplete migration, and slow or erratic movements. As a result, the mispositioned epidermal cells observed in *sax-3* animals could reflect an indirect consequence of the failure of neuroectoblast (AB lineage) movement earlier in development. This is supported by the observation that expression of *F25B3.3*::SAX-3 in neuroblasts was able to partially rescue the *sax-3* defects. However, the ability of *ajm-1*::SAX-3 to rescue *sax-3* embryonic lethality clearly indicates that SAX-3 could function autonomously in epidermal cells.

The lethality in both *sax-3* and *vab-1* embryos was caused by a defect in cell movements and not as a result of defective cell differentiation. For example, the structure of the pharynx and intestine were formed correctly in Class I terminal-stage *vab-1* and *sax-3* embryos, and the GABAergic motoneurons and mechanosensory neurons were specified and expressed using the *unc-25*::GFP and *mec-4*::GFP markers, respectively (data not shown). The body muscles were also differentiated judging by the presence of muscle twitching in terminal stage mutants.
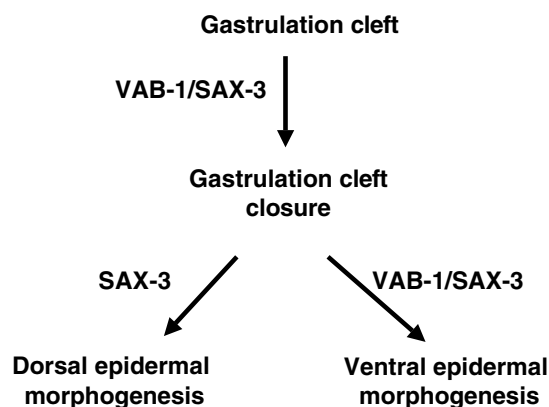
Significance of the interaction between VAB-1 Eph Tyrosine Kinase and the juxtamembrane CC1 region of SAX-3/Robo

The Robo receptor family is characterized by an extracellular domain consisting of two to five immunoglobulin domains and two to three fibronectin type III repeats, and a cytoplasmic domain containing various combinations of four short **C**onserved **C**ytoplasmic motifs called CC0, CC1, CC2 and CC3 (Bashaw et al., 2000; Kidd et al., 1998). These motifs are thought to serve as binding sites for various intracellular signaling molecules, including Enabled (Ena) and the Ableson (Abl) tyrosine kinase (Bashaw et al., 2000). We have shown an interaction between the VAB-1 tyrosine kinase domain and the juxtamembrane and CC1 region of SAX-3/Robo. SAX-3 does not have a CC0 consensus, which is located in the juxtamembrane region of Robo receptors; however, there are seven tyrosine residues in the SAX-3 juxtamembrane region that VAB-1 could potentially phosphorylate. Interestingly, the

human and mouse Robo3/RIG-1 lacks the CC1 domain and differs from the other Robo homologs because it is required for midline crossing, which is opposite to the role of Robo receptors. It appears to accomplish this by repressing Robo1/2 signaling (Sabatier et al., 2004). Thus, the CC1 region may be important in regulating a repulsive signaling downstream of Robo. It will be of interest to determine whether VAB-1 phosphorylates SAX-3 to alter its function, or whether the SAX-3/VAB-1 interaction affects the UNC-40/SAX-3 interaction or the ability of Abl to regulate SAX-3/Robo function.

SAX-3/Robo functions independently of VAB-1 and has the potential to form neuronal receptor complexes with the VAB-1 Eph RTK

We propose a model in which SAX-3 has two cooperative roles. The first is to function together with VAB-1 in AB neuroectoblast movement during late gastrulation and ventral enclosure to provide a substrate or a signal for proper epidermal cell movements specifically on the ventral side of the embryo. A second role for SAX-3 may be to function independently of VAB-1 in the epidermis for epidermal movements. For example, on the dorsal side, because *sax-3* animals display dorsal epidermal defects that are not shared by the *vab-1* null (Fig. 7). Similarly, *sax-3* animals display axon guidance defects not seen in *vab-1* mutants, suggesting that SAX-3 has VAB-1-independent roles during axon development (Zallen et al., 1999). This is also consistent with their expression patterns, where SAX-3 and VAB-1 are co-expressed early in development but later are expressed in separate cells. George et al. showed by genetic mosaic analysis that loss of *vab-1* in AB lineages caused strong morphogenetic defects, including the 'notched-head' epidermal defect (George et al., 1998). Similarly, the *sax-3* 'notched-head' defects could arise

Gastrulation cleft

VAB-1/SAX-3 ↓

Gastrulation cleft closure

SAX-3 ↙   ↘ VAB-1/SAX-3

Dorsal epidermal morphogenesis   **Ventral epidermal morphogenesis**

Fig. 7. Model for the function of SAX-3 in *C. elegans* embryonic development. During embryonic development most cells reach their final position through a combination of local divisions and directed movements. SAX-3/VAB-1 pathways are required for neuroblast movements that result in the closing of the gastrulation cleft. SAX-3/VAB-1 may also be required to position early AB epidermal precursors that will generate the future epidermal seam cells and ventral epidermal cells. Our results are consistent with SAX-3 functioning with VAB-1 in parallel pathways or perhaps through a receptor complex (SAX-3/VAB-1). At the same time SAX-3 functions independently of VAB-1 for epidermal morphogenesis; for example, during the migration of dorsal epidermal cells.

as a result of a requirement for SAX-3 in the AB lineages, as *F25B3.3*::SAX-3 expression in the AB neuroectoblast specifically rescues this defect; by contrast, the *ajm-1*::SAX-3 expression in epidermal cells did not rescue the epidermal notched-head defect. Furthermore, the double *vab-1; sax-3* mutants do not exhibit any new phenotype over those observed in single mutants, suggesting that SAX-3 and VAB-1 have common and partially redundant functions during morphogenetic movements.

In vitro binding of the VAB-1 kinase domain, and the juxtamembrane and CC1 region of SAX-3, support the formation of a co-receptor complex between VAB-1 and SAX-3. Non-allelic, non-complementation and a gene-dosage requirement for VAB-1 in the absence of the SAX-3/Robo receptor also provide genetic evidence to support the formation of a complex between VAB-1 and SAX-3. Proteins that physically interact with Robo receptors appear to be sensitive to dosage or show non-allelic non-complementation. For example, in *Drosophila*, null mutations in the *slit* ligand fail to complement null alleles of *Robo* (Kidd et al., 1999), and *Robo* mutants dominantly enhance *Vilse*, which encodes a Rac/Cdc42 GAP (Lundstrom et al., 2004) and binds *Robo* specifically at the CC2 region. In *C. elegans*, removing a single copy of UNC-34/enabled, an interacting effector of SAX-3/Robo signaling, significantly enhances the nerve ring phenotypes of a weak allele of *sax-3* (Yu et al., 2002). Robo receptors have been reported to have the potential to form homodimers, as well as heterodimers with the Netrin receptor UNC-40/DCC (Hivert et al., 2002; Stein and Tessier-Lavigne, 2001; Yu et al., 2002). What is the significance of a SAX-3/VAB-1 receptor complex? The Robo receptors do not have any apparent catalytic activity and thus the association of VAB-1 Eph RTK and SAX-3/Robo may provide SAX-3/Robo with a different function than when it signals independently. In *C. elegans* there is only one Robo receptor, whereas in *Drosophila* there are three and in vertebrates there are at least four Robo homologs. A combinatorial code of Robo receptors has been proposed where various homo- and heterodimeric combinations of Robo, Robo2 and Robo3 can determine axon trajectory in the *Drosophila* CNS (Rajagopalan et al., 2000; Simpson et al., 2000). Because *C. elegans* possesses only one Robo receptor, this combinatorial code does not exist per se, therefore the interaction with other receptors, such as VAB-1 Eph RTK, may provide the signaling diversity required during development. The *sax-3* and *vab-1* genetic interactions are reminiscent of the *unc-5* and *unc-40* genes in hermaphrodite distal tip cell (DTC) migration. These two genes encode Netrin receptors that can function either independently or together for repulsion in the hermaphrodite gonad distal tip cells (Hong et al., 1999; Merz et al., 2001).

The vertebrate Robo receptors and Eph RTKs have been shown to mediate axonal repulsion, and in some cases to work in the same neurons. It has even been suggested that the downstream signaling between these two neuronal receptors converge on phosphatidylinositol-3-kinase (PI3K) signaling (Wong et al., 2004). The vertebrate Eph RTKs have also been shown to function during angiogenesis, and, curiously, Magic Roundabout (Robo4) is expressed specifically in the vasculature and is essential for angiogenesis (Bedell et al., 2005; Suchting et al., 2005). It will be interesting to know whether in other organisms the Eph RTKs and Robo receptors

work together in a similar fashion to that which we propose for the early morphogenetic movements in *C. elegans*.

References

Adams, R. H. and Klein, R. (2000). Eph receptors and ephrin ligands. Essential mediators of vascular development. *Trends Cardiovasc. Med.* **10**, 183-188.

Altun-Gultekin, Z., Andachi, Y., Tsalik, E. L., Pilgrim, D., Kohara, Y. and Hobert, O. (2001). A regulatory cascade of three homeobox genes, *ceh-10*, *ttx-3* and *ceh-23*, controls cell fate specification of a defined interneuron class in *C. elegans*. *Development* **128**, 1951-1969.

Ausubel, F. M., Brent, R., Kingston, R. E., Moore, D. D., Seidman, J. G., Smith, J. A. and Struhl, K. (1989). *Current Protocols in Molecular Biology*. New York: Wiley-Interscience.

Bashaw, G. J., Kidd, T., Murray, D., Pawson, T. and Goodman, C. S. (2000). Repulsive axon guidance: Abelson and Enabled play opposing roles downstream of the Roundabout receptor. *Cell* **101**, 703-715.

Bedell, V. M., Yeo, S. Y., Park, K. W., Chung, J., Seth, P., Shivalingappa, V., Zhao, J., Obara, T., Sukhatme, V. P., Drummond, I. A. et al. (2005). roundabout4 is essential for angiogenesis in vivo. *Proc. Natl. Acad. Sci. USA* **102**, 6373-6378.

Brenner, S. (1974). The genetics of *Caenorhabditis elegans*. *Genetics* **77**, 71-94.

Brose, K., Bland, K. S., Wang, K. H., Arnott, D., Henzel, W., Goodman, C. S., Tessier-Lavigne, M. and Kidd, T. (1999). Slit proteins bind Robo receptors and have an evolutionarily conserved role in repulsive axon guidance. *Cell* **96**, 795-806.

Challa, A. K., Beattie, C. E. and Seeger, M. A. (2001). Identification and characterization of roundabout orthologs in zebrafish. *Mech. Dev.* **101**, 249-253.

Chin-Sang, I. D., George, S. E., Ding, M., Moseley, S. L., Lynch, A. S. and Chisholm, A. D. (1999). The ephrin VAB-2/EFN-1 functions in neuronal signaling to regulate epidermal morphogenesis in C. elegans. *Cell* **99**, 781-790.

Chin-Sang, I. D., Moseley, S. L., Ding, M., Harrington, R. J., George, S. E. and Chisholm, A. D. (2002). The divergent C. elegans ephrin EFN-4 functions inembryonic morphogenesis in a pathway independent of the VAB-1 Eph receptor. *Development* **129**, 5499-5510.

Dodelet, V. C. and Pasquale, E. B. (2000). Eph receptors and ephrin ligands: embryogenesis to tumorigenesis. *Oncogene* **19**, 5614-5619.

Drescher, U. (2000). Eph receptor tyrosine kinases and their ligands in development. *Ernst Schering Res. Found. Workshop* **29**, 151-164.

Edgley, M. L. and Riddle, D. L. (2001). LG II balancer chromosomes in Caenorhabditis elegans: mT1(II;III) and the mIn1 set of dominantly and recessively marked inversions. *Mol. Genet. Genomics* **266**, 385-395.

Finney, M. and Ruvkun, G. (1990). The *unc-86* gene product couples cell lineage and cell identity in *C. elegans*. *Cell* **63**, 895-905.

Flanagan, J. G. and Vanderhaeghen, P. (1998). The ephrins and Eph receptors in neural development. *Annu. Rev. Neurosci.* **21**, 309-345.

Francis, R. and Waterston, R. H. (1991). Muscle cell attachment in Caenorhabditis elegans. *J. Cell Biol.* **114**, 465-479.

George, S. E., Simokat, K., Hardin, J. and Chisholm, A. D. (1998). The VAB-1 Eph receptor tyrosine kinase functions in neural and epithelial morphogenesis in C. elegans. *Cell* **92**, 633-643.

Hao, J. C., Yu, T. W., Fujisawa, K., Culotti, J. G., Gengyo-Ando, K., Mitani, S., Moulder, G., Barstead, R., Tessier-Lavigne, M. and Bargmann, C. I. (2001). C. elegans Slit acts in midline, dorsal-ventral, and anterior-posterior guidance via the SAX-3/Robo Receptor. *Neuron* **32**, 25-38.

Harrington, R. J., Gutch, M. J., Hengartner, M. O., Tonks, N. K. and Chisholm, A. D. (2002). The C. elegans LAR-like receptor tyrosine phosphatase PTP-3 and the VAB-1 Eph receptor tyrosine kinase have partly redundant functions in morphogenesis. *Development* **129**, 2141-2153.

Hivert, B., Liu, Z., Chuang, C. Y., Doherty, P. and Sundaresan, V. (2002). Robo1 and Robo2 are homophilic binding molecules that promote axonal growth. *Mol. Cell. Neurosci.* **21**, 534-545.

Hobert, O. (2002). PCR fusion-based approach to create reporter gene constructs for expression analysis in transgenic C. elegans. *Biotechniques* **32**, 728-730.

Hong, K., Hinck, L., Nishiyama, M., Poo, M. M., Tessier-Lavigne, M. and Stein, E. (1999). A ligand-gated association between cytoplasmic domains of UNC5 and DCC family receptors converts netrin-induced growth cone attraction to repulsion. *Cell* **97**, 927-941.

Kidd, T., Brose, K., Mitchell, K. J., Fetter, R. D., Tessier-Lavigne, M., Goodman, C. S. and Tear, G. (1998). Roundabout controls axon crossing of the CNS midline and defines a novel subfamily of evolutionarily conserved guidance receptors. *Cell* **92**, 205-215.

Kidd, T., Bland, K. S. and Goodman, C. S. (1999). Slit is the midline repellent for the Robo receptor in Drosophila. *Cell* **96**, 785-794.

Kullander, K. and Klein, R. (2002). Mechanisms and functions of Eph and ephrin signalling. *Nat. Rev. Mol. Cell Biol.* **3**, 475-486.

Lee, J. S., Ray, R. and Chien, C. B. (2001). Cloning and expression of three zebrafish roundabout homologs suggest roles in axon guidance and cell migration. *Dev. Dyn.* **221**, 216-230.

Lundstrom, A., Gallio, M., Englund, C., Steneberg, P., Hemphala, J., Aspenstrom, P., Keleman, K., Falileeva, L., Dickson, B. J. and Samakovlis, C. (2004). Vilse, a conserved Rac/Cdc42 GAP mediating Robo repulsion in tracheal cells and axons. *Genes Dev.* **18**, 2161-2171.

Mello, C. C., Kramer, J. M., Stinchcomb, D. and Ambros, V. (1991). Efficient gene transfer in *C. elegans*: extrachromosomal maintenance and integration of transforming sequences. *EMBO J.* **10**, 3959-3970.

Merz, D. C., Zheng, H., Killeen, M. T., Krizus, A. and Culotti, J. G. (2001). Multiple signaling mechanisms of the UNC-6/netrin receptors UNC-5 and UNC-40/DCC in vivo. *Genetics* **158**, 1071-1080.

Mohler, W. A., Simske, J. S., Williams-Masson, E. M., Hardin, J. D. and White, J. G. (1998). Dynamics and ultrastructure of developmental cell fusions in the Caenorhabditis elegans hypodermis. *Curr. Biol.* **8**, 1087-1090.

Podbilewicz, B. and White, J. G. (1994). Cell fusions in the developing epithelia of *C. elegans*. *Dev. Biol.* **161**, 408-424.

Rajagopalan, S., Nicolas, E., Vivancos, V., Berger, J. and Dickson, B. J. (2000). Crossing the midline: roles and regulation of Robo receptors. *Neuron* **28**, 767-777.

Riddle, D. L., Blumenthal, T., Meyer, B. J. and Priess, J. R. (1997). C. Elegans *II*. Plainview, New York: Cold Spring Harbor Laboratory Press.

Sabatier, C., Plump, A. S., Le Ma, Brose, K., Tamada, A., Murakami, F., Lee, E. Y. and Tessier-Lavigne, M. (2004). The divergent Robo family protein Rig-1/Robo3 is a negative regulator of Slit responsiveness required for midline crossing by commissural axons. *Cell* **117**, 157-169.

Schiestl, R. H. and Gietz, R. D. (1989). High efficiency transformation of intact yeast cells using single stranded nucleic acids as a carrier. *Curr. Genet.* **16**, 339-346.

Seeger, M., Tear, G., Ferres-Marco, D. and Goodman, C. S. (1993). Mutations affecting growth cone guidance in Drosophila: genes necessary for guidance toward or away from the midline. *Neuron* **10**, 409-426.

Serebriiskii, I. G. and Golemis, E. A. (2000). Uses of lacZ to study gene function: evaluation of beta-galactosidase assays employed in the yeast two-hybrid system. *Anal. Biochem.* **285**, 1-15.

Sherman, F. (1991). Getting started with yeast. *Methods Enzymol.* **194**, 3-21.

Simpson, J. H., Bland, K. S., Fetter, R. D. and Goodman, C. S. (2000). Short-range and long-range guidance by Slit and its Robo receptors: a combinatorial code of Robo receptors controls lateral position. *Cell* **103**, 1019-1032.

Stein, E. and Tessier-Lavigne, M. (2001). Hierarchical organization of guidance receptors: silencing of netrin attraction by slit through a Robo/DCC receptor complex. *Science* **291**, 1928-1938.

Suchting, S., Heal, P., Tahtis, K., Stewart, L. M. and Bicknell, R. (2005). Soluble Robo4 receptor inhibits in vivo angiogenesis and endothelial cell migration. *FASEB J.* **19**, 121-123.

Sulston, J. E., Schierenberg, E., White, J. G. and Thomson, J. N. (1983). The embryonic cell lineage of the nematode *Caenorhabditis elegans*. *Dev. Biol.* **100**, 64-119.

Williams-Masson, E. M., Heid, P. J., Lavin, C. A. and Hardin, J. (1998). The cellular mechanism of epithelial rearrangement during morphogenesis of the Caenorhabditis elegans dorsal hypodermis. *Dev. Biol.* **204**, 263-276.

Wong, E. V., Kerner, J. A. and Jay, D. G. (2004). Convergent and divergent signaling mechanisms of growth cone collapse by ephrinA5 and slit2. *J. Neurobiol.* **59**, 66-81.

Wong, K., Park, H. T., Wu, J. Y. and Rao, Y. (2002). Slit proteins: molecular guidance cues for cells ranging from neurons to leukocytes. *Curr. Opin. Genet. Dev.* **12**, 583-591.

Yu, T. W., Hao, J. C., Lim, W., Tessier Lavigne, M. and Bargmann, C. I. (2002). Shared receptors in axon guidance: SAX-3/Robo signals via UNC-34/Enabled and a Netrin-independent UNC-40/DCC function. *Nat. Neurosci.* **5**, 1147-1154.

Zallen, J. A., Yi, B. A. and Bargmann, C. I. (1998). The conserved immunoglobulin superfamily member SAX-3/Robo directs multiple aspects of axon guidance in *C. elegans. Cell* **92**, 217-227.

Zallen, J. A., Kirch, S. A. and Bargmann, C. I. (1999). Genes required for axon pathfinding and extension in the *C. elegans* nerve ring. *Development* **126**, 3679-3692.